

Antioxidant Assay Based on Quenching of Photocatalytically Generated Reactive Oxygen Species

JIA Rui-Jie¹, ZHANG Qiang², LIU Ji-Feng^{1,2,*}, Mohamad Hojeij³, Hubert H. Girault^{3,*}



¹ Department of Chemistry, Liaocheng University, Liaocheng 252059, China.

² Key Laboratory of Food Nutrition and Safety, Ministry of Education of China, Tianjin University of Science and Technology, Tianjin 300457, China

³ Laboratoire d'Electrochimie Physique et Analytique, Station 6, Ecole Polytechnique Fédérale de Lausanne, CH-1015, Lausanne, Switzerland

Abstract: A method based on photogeneration of OH radicals in water from TiO₂ nanoparticles was developed to study the kinetics of oxidation of organic molecules which were used as biological antioxidants. The kinetics of oxidation of terephthalic acid as a reference probe was monitored by fluorescence measurements of the concentration of its oxidized form, 2-hydroterephthalic acid ($\lambda_{\text{ex}} = 315$ nm, $\lambda_{\text{em}} = 425$ nm). The kinetics of oxidation of other antioxidant molecules was then deduced from the radical scavenging competition. The antioxidant properties of normal antioxidants were compared based on this kinetic model. And the antioxidant kinetic decreased in the order: lipoic acid, gallic acid, glutathione, uric acid, vitamin C, vitamin E, trolox and bilirubin.

Key Words: Reactive oxygen species; Bioantioxidants; Photocatalysis; Reaction kinetics

1 Introduction

Bio-oxidation processes and the role of antioxidants (AOs) in life sciences are widely recognized as a central issue of modern biology. Oxidative metabolisms are the main energy providers in biological systems and are essential for the survival of cells. During these metabolic processes, free radicals and other reactive oxygen species (ROS) are generated and may cause oxidative damages^[1]. When excess free radicals or ROS overwhelm the antioxidant protagonists, including the endogenous protective enzymes (e.g., superoxide dismutase, catalase and peroxidase), the endogenous sacrificial molecules (e.g., glutathione) or the exogenous dietary substances (e.g., vitamin C, E), the destructive and lethal cellular effects would occur. Therefore, it is of fundamental importance to understand and control the oxidative stress.

According to a mechanistic viewpoint, the antioxidants can be oxidized either by hydrogen atom acceptors (e.g., ROO[•]) or by electrons acceptors (e.g., Fe³⁺). Different methods were

proposed to study the antioxidant properties of molecules acting through the radical reaction pathway, whereby the antioxidant and the substrate compete for thermally generating peroxy radicals. These methods used absorbance or fluorescent indicators with different parameters to evaluate the antioxidant properties^[1,2]. Among these methods, the total radical trapping antioxidant parameter (TRAP)^[3], the oxygen radical absorbance capacity (ORAC)^[4], and the 2,2-diphenyl-1-picrylhydrazyl (DPPH) radical scavenging capacity^[5] were described in detail. Generally, these assays employ both a radical initiator and a molecular probe (UV or fluorescence) to monitor the reaction's progress and the antioxidant capacity by using the analysis of the reaction kinetics. The radical scavenging capacity directly relates to the hydrogen atom donating ability of the antioxidants, so that it is usually used as a parameter to quantify the antioxidant capacity. In these assays, the concentration of the probe is often lower than that of the antioxidants. This differs from biological conditions where the antioxidant concentration is usually lower than that of the substrate (biological molecular or cell targets). In

Received 22 October 2015; accepted 21 March 2016

*Corresponding author. Email: jfliu@tust.edu.cn, hubert.girault@epfl.ch

This work was supported by the National Natural Science Foundation of China (Nos. 21127006, 21575102).

Copyright © 2016, Changchun Institute of Applied Chemistry, Chinese Academy of Sciences. Published by Elsevier Limited. All rights reserved.

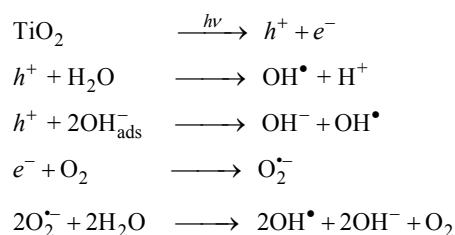
DOI: 10.1016/S1872-2040(16)60950-7

addition, trolox equivalent antioxidant capacity (TEAC)^[6] method and ferric ion reducing antioxidant power (FRAP) method were also proposed to study the antioxidant properties of molecules acting through the electron transfer pathway^[7].

Recently, the OH radical quenching^[8], H₂O₂ quenching^[9], H₂O₂ and OH radical quenching^[10] electrochemical methods were reported for the antioxidant test, and different kinetic models were developed to compare the antioxidant activity. Niu's group developed antioxidant test methods based on quenching photocatalytic generated species (e.g., positive holes and ROS)^[11–13]. On the basis of this, we established a kinetic model for this photoelectrochemical detection technique for antioxidant test.

Biologically speaking, OH radicals are generated when H₂O₂ reacts with Fe(II) (Fenton type reaction)^[14,15]. However, the use of Fenton reaction mixtures has disadvantages in scavenging assays because many antioxidants are also metal chelators that alter the activity of Fe(II) after chelation. Antioxidants at high concentration may act as pro-oxidant to enhance the generation of OH radicals^[16]. These secondary factors complicate the determination of the OH radicals scavenging capacity of the antioxidants. In comparison, we demonstrated that the photocatalytic oxidation of water by TiO₂ nanoparticles was a clean and straightforward method to reproducibly generate OH radicals for antioxidant studies^[17].

Recently, TiO₂ nanostructured materials have been applied in many fields, such as solar energy conversion, water splitting, environmental decontamination, and so on^[18–22]. The electronic structure of TiO₂ includes a full valence band (VB) and empty conduction (CB), and there is a bandgap (E_g) of 3.2 eV^[19] between the two. When the energy illuminated by a photon matches or exceeds the band gap, an electron is excited from the valence band into the conduction band, leaving a positive hole in the valence band. In the presence of electron donors and acceptors in solution, the recombination reaction between the electron and the hole can be prevented by redox reactions. As shown in Scheme 1, in the photolysis of TiO₂ in pure water, the solvating nanoparticles of water molecules and the dissolved O₂ can react with both the hole and the electron respectively to generate OH radicals. This photocatalytic reaction of TiO₂ was already successfully applied to the design of an antioxidant sensor based on ds-DNA modified TiO₂ electrodes. A ds-DNA layer was adsorbed on a TiO₂



Scheme 1 Photochemical reactions of TiO₂ in water layer deposited on an indium tin oxide (ITO) electrode. Upon

irradiation of the electrode, the produced OH radicals oxidized the adsorbed DNA and the resulting ds-DNA damage was measured using redox intercalators^[8].

In the present work, by using terephthalic acid (TA) as an oxidation probe and hydroxy-terephthalic acid (HTA) generated in the photolysis of TiO₂ nanoparticles in solution as a fluorescent probe, a scavenging antioxidant capacity assay was carried out for the oxidation kinetic analysis of AOs based on the competing reaction of TA and AOs with HTA.

2 Materials and methods

2.1 Reagents and solutions

The phosphate buffer solution (PBS) was made of sodium phosphate (Na₂HPO₄:NaH₂PO₄ = 81:19, molar ratio) and NaCl dissolved in water at a final concentration of 50 and 10 mM, respectively (pH 7.4). Glutathione (Sigma), gallic acid (Acros), vitamin C (Riedel-de Haën), uric acid (Fluka), trolox (Fluka), bilirubin (Fluka), micellated lipoic acid (Degussa) were dissolved in PBS. Vitamin E (*D,L*- α -tocopherol acetate, Sigma) was dissolved in 0.1% Triton X-100 at a concentration of 10 mM. These chemicals were used as model antioxidants. TiO₂ nanoparticles (Degussa, P25, 21 nm in diameter, 50 m² g⁻¹) were kindly provided by Dr. John Kiwi (LPI-ISIC-EPFL). To break the aggregates into separate particles, the TiO₂ powder was ground in a porcelain mortar with a small amount of water and finally suspended into aqueous solution (0.5 mg mL⁻¹). TA (Fluka) stock solution (1 mM) was prepared by dissolving a certain amount of TA into 2 mM NaOH aqueous solution.

2.2 Fluorescence emission

The fluorescence spectra of HTA (generated by the reaction of TA with OH radical) were measured on a Perkin-Elmer LS-50B fluorescence spectrometer. Antioxidant solutions were mixed with TiO₂ (25 $\mu\text{g mL}^{-1}$) and TA (0.1 mM) and illuminated using a UV lamp with a peak wavelength at 360 nm during a given time. After irradiation, the solution was transferred for fluorescence measurements. For the fluorescence emission experiments, the excitation wavelength was set at 315 nm and the signal was recorded at 425 nm.

2.3 Fluorescence lifetime measurements

The fluorescence lifetime decay measurements were performed using the time-correlated single photon counting (TCSPC) technique. Femtosecond laser pulses from a mode locked Ti: sapphire laser (Spectra Physics, Tsunami), pumped by a Nd:YVO₄ solid state laser (Spectra Physics, Millennia Xs), were directed to a pulse picker and frequency doubler (Spectra Physics, model 3980). For the present study, the

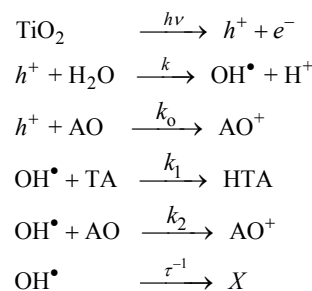
repetition rate was set at 400 kHz. The excitation laser beam was *s*-polarized using a polarizer. The fluorescence was focused by a lens placed at a 90° angle from the excitation beam to the entrance slit of a monochromator (Jobin Yvon, H-10) and detected by a cooled microchannel plate photomultiplier (MCP-PM, Hamamatsu, R3809U-50). The temperature of the MCP-PM housing was set at -20 °C to minimize the dark counts from the MCP-PM. The output of the MCP-PM was further amplified using an amplifier (Becker & Hickl GmbH) and analyzed by a single photon counting module (Edinburgh Instruments, TCC900). The constant fraction discriminator (CFD) parameters were optimized using T900 software to obtain the best fit and lifetimes for the fluorescence lifetime standard molecules. The overall instrumental response function, as recorded by scattering the excitation light using Ludox in a sample cell, was around 90 ps full width at half maximum. The laser pulse STOP synchronization was performed by using the laser fundamental beam from the pulse picker and detected using optical trigger OT900 (15 V bias, rise-time 450 ps). The fluorescence-monitoring wavelength was set at 425 nm throughout the study. The number of the fluorescent photons was kept low relatively to the number of start pulses (1% or less).

3 Results and discussion

3.1 Fluorescence measurements

Fluorescence spectrometer was used to monitor the formation of fluorescent 2-hydroxyterephthalic acid (HTA) following the scavenging of OH radicals by TA and the addition reaction on the benzene ring^[23], as shown in Scheme 2. In the reaction, AOs competed with TA for the formation and scavenging of the photogenerated OH radicals and inhibited the formation of HTA. So the fluorescence of HTA was monitored to assay the antioxidant capacity of antioxidants. The schematic diagram of the method was shown in Fig.1.

The fluorescence emission spectra recorded for a solution of TA containing TiO₂ nanoparticles after irradiation by UV light for different lengths of time is illustrated in Fig.2. Gradual increases in the fluorescence at 425 nm were observed, and the emission intensity recorded at this wavelength was proportional to the illumination time at suitable TA concentrations. The observed fluorescence signal originated from HTA molecules in solution. Of course, it is known that TA binds to TiO₂ nanoparticles with an association constant of 10⁵ [24]. However, neither surface bound TA nor HTA are expected to fluoresce, as it is usually difficult to observe the fluorescence from chromophores bound to TiO₂. To verify this point, the nanoparticles was separated from the solution by centrifugation, and the fluorescence spectra of the solution and the particles re-dispersed in water



Scheme 2 Photochemical reactions of TiO₂ in water in the presence of TA and AOs

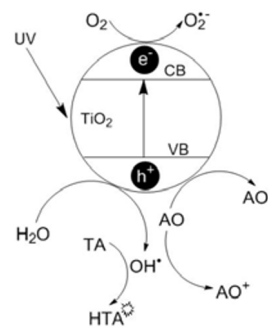


Fig.1 Schematic diagram of OH radicals scavenging capacity assay TA, terephthalic acid; HTA, 2-hydroxyterephthalic acid; AO, antioxidant

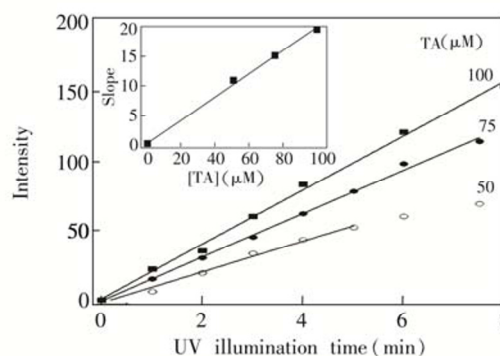


Fig.2 Fluorescence intensity of TA at different concentrations Concentration of TiO₂: 25 μg mL⁻¹, Inset: k^{-1} vs [TA]_{tot}

were measured, and no obvious emission was observed for surface bound HTA. Figure 3 showed the fluorescence lifetime decay profile for HTA in PBS solution with an excitation wavelength of 350 nm and emission wavelength of 425 nm. The decay profile of HTA could be reasonably well fitted with a double exponential model:

$$I(t) = A_1 e^{-t/\tau_1} + A_2 e^{-t/\tau_2} \quad (1)$$

where, τ_1 and τ_2 were the shorter and longer lifetime components respectively, and A_1 and A_2 were the corresponding amplitudes. The fit parameters were presented in Table 1. These data in Table 1 showed that the fluorescence signal monitored in Fig.2 stemmed from the oxidation of unbound species. This result was identical with the observation results of Nosaka *et al*^[25]. In Nosaka's work, they compared the quantum efficiencies of OH radicals that obtained by 4-carboxy-2,2,6,6-

Table 1 Fluorescence decay fit parameters of HTA in PBS solution

| | | | |
|------------|-----------------------|-------|-------|
| τ_1 | 1.048 ± 0.025 ns | A_1 | 0.107 |
| τ_2 | 12.183 ± 0.257 ns | A_2 | 0.668 |
| γ_0 | 0.0013 | x_2 | 1.038 |

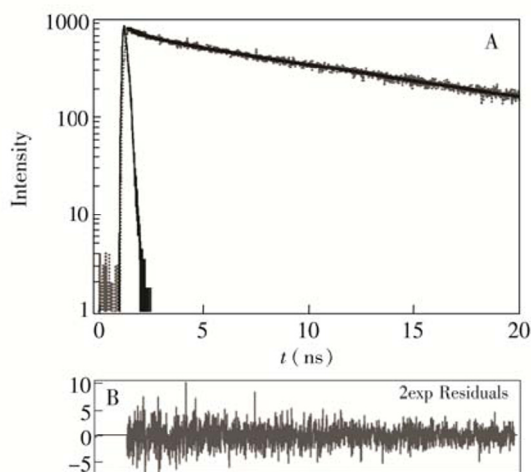


Fig.3 HTA Fluorescence decay including the instrument response, fitted function (top) and residuals for double exponential fit (bottom). The excitation and detection wavelength were 325 and 425 nm, respectively. $[HTA] \leq 100 \mu M$ in PBS buffer solution

tetramethylpiperidine-1-oxyl (CTMPO) spin probe method, respectively, and thought that the free HTA could react with OH radical in solution^[25].

3.2 Kinetic analysis

In the presence of antioxidants (AOs), the production rate of HTA decreased as the OH radicals were also scavenged by AOs in PBS solution. A simple kinetic model is proposed to quantify the OH scavenging capacities of AOs based on the reactions of Scheme 2. Where k is the pseudo-first order generation rate constants of OH radicals by oxidation of water, k_0 is the rate constant for the direct oxidation of antioxidants by photogenerated holes and k_1 , k_2 are the reaction rate constants for the oxidation of TA and antioxidants with OH radicals. The last reaction is a pseudo-first order (τ^{-1}) one corresponding to the lifetime of hydroxyl radicals in aqueous solutions. The incident photon-to-electron conversion efficiency (IPCE) is a function of the absorptivity A , i.e. the fraction of the incident light that is absorbed by the solution, a function of the quantum yield for the photogeneration of electron-hole pairs, and a function of the incoming light intensity, as shown in the following equation:

$$IPCE = A\phi I \quad (2)$$

The quantum yield for hole generation was measured to be of the order of 10^{-2} , which was a typical value for a photocatalytic of magnitude reaction^[26]. In water according to

the scheme above, the quantum yield for OH radical production was $\Phi_{OH} = kA\phi I$. By monitoring the oxidation of TA, the quantum yield was detected to be 7×10^{-5} ^[26]. When only TA was presented in the solution, the steady-state approximation for the holes and the OH radicals was described as the following equation.

$$[OH] = A\phi I / (k_1[TA] + \tau^{-1}) \quad (3)$$

where, $[TA]$ represents the bulk concentration of unbound TA. At the beginning of the UV illumination and within a short time scale, the concentration of TA could be considered constant and the production rate of HTA was then directly proportional to the illumination time.

$$[HTA] = A\phi I k_1 [TA] t / (k_1 [TA] + \tau^{-1}) = k^1 t \quad (4)$$

where, k^1 represents the pseudo-first order rate constant for the production of HTA. The fluorescence intensity varies linearly with increasing UV illumination time when TA is in excess as predicted by Eq.(4). Since k^1 varies also linearly with the total TA concentration at least at short illumination times, Eq.(4) can be approximated by an equation as follows:

$$[HTA] = A\phi I k_1 [TA] \tau t = k^1 t \quad (5)$$

which shows that most of the OH^{*} radicals produced are scavenged by the solvent rather than by TA. For the rest of this work, the TA concentration was fixed to 100 μM and the pseudo-first order k^1 for this concentration was measured to be 19.6 min^{-1} .

In the presence of AOs, the steady-state approximation for OH radical is described according to Eq.(6).

$$d[OH^*]/dt = k[h^+] - k_1[OH^*][TA] - k_2[OH^*][AO] - \tau[OH^*] \quad (6)$$

And the steady-state approximation for the photogenerated hole is described according to Eq.(7).

$$d[h^+]/dt = A\phi I - k[h^+] - k_0[AO][h^+] \quad (7)$$

On a short time scale, the concentration of AO can also be treated as a constant and the production rate of HTA is as follows:

$$[HTA] = [A\phi I k / (k + k_0[AO])] [k_1[TA] / (k_1[TA] + k_2[AO] + \tau^{-1})] t = k^1_{OA} t \quad (8)$$

The fluorescence intensity of HTA varies linearly with the UV illumination time, and the apparent pseudo-first order rate constant k^1_{OA} decreases with the increase of concentration AO. These data validated the kinetic model proposed above. Assuming that the rate of direct oxidation of AO on TiO₂ nanoparticles is smaller than that of the oxidation of water, and $k_1[TA] \ll \tau^{-1}$ in Eq.(4), Eq.(8) can be reduced to Eq.(9):

$$[HTA] = A\phi I k_1 [TA] t / (k_2[AO] + \tau^{-1}) = k^1_{OA} t \quad (9)$$

The reciprocal of k^1_{OA} is then proportional to AO concentrations as shown in Fig.4.

$$[k^1_{OA}]^{-1} = (k^1)^{-1} + k_2 \tau [AO] / k^1 \quad (10)$$

As shown in in Fig.4, the obtained antioxidant concentration can be used to characterize the antioxidant capacities of the different molecules, and the larger the slope is observed, the higher antioxidant capacity is obtained. So, the parameter $k_2 \tau$ can be used to quantify the antioxidant capacity of a given molecule.

These data showed that the compound concentrations which could be used for the competing reaction with 100 μM

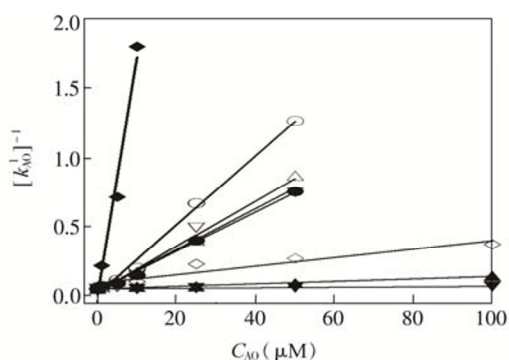


Fig.4 Plotting of Eq.(10) ($[k_{OA}^1]^{-1}$ vs [AO])

◆, lipoic acid; ○, gallic acid; △, glutathione; ▽, uric acid; ●, vitamin C; ◇, vitamin E; ▲, trolox; ▼, bilirubin. [TA] = 0.1 mM

TA in water were 114 μM for lipoic acid, 770 μM for gallic acid, 1.2 mM for glutathione, 1.3 mM for uric acid, 1.4 mM for vitamin C, 6.5 mM for vitamin E, 30 mM for trolox and 100 mM for bilirubin, respectively. However, it should be emphasized that the methodology presented above could be applied to the analysis of antioxidant capacity of water-soluble AOs, but not for the analysis of macromolecules such as bovine serum albumin that binds and coats the TiO_2 nanoparticles.

4 Conclusions

The present investigation demonstrated that the use of TiO_2 nanoparticles in conjunction with the photo-oxidation of TA was ideally suited to assay the antioxidant properties of small molecules in aqueous solutions. The method provided an easy method to generate OH radicals compared to the pulse radiolysis techniques or the methods based on the Fenton reaction, and can be used for the high-throughput analysis of AOs by combining with microtiter plate method and fluorescence detector.

References

- [1] Antolovich M, Prenzler P D, Patsalides E, McDonald S, Robards K. *Analyst*, **2002**, 127(1): 183–198
- [2] Huang D, Ou B, Prior R L. *J. Agric. Food Chem.*, **2005**, 53(6): 1841–1856
- [3] Wayner D D M, Burton G W, Ingold K U, Locke S. *FEBS Lett.*, **1985**, 187(1): 33–37
- [4] Cao G H, Alessio H M, Cutler R G. *Free Radical Biol. Med.*, **1993**, 14(3): 303–311
- [5] Blois M S. *Nature*, **1958**, 181(4617): 1199–1200
- [6] Miller N J, Rice-Evans C A, Davies M J, Gopinathan V, Milner A. *Clin. Sci.*, **1993**, 84(4): 407–412
- [7] Benzie I F F, Strain J J. *Anal. Biochem.*, **1996**, 239(1): 70–76
- [8] Liu J, Roussel C, Lagger G, Tacchini P, Girault H H. *Anal. Chem.*, **2005**, 77(23): 7687–7694
- [9] Guo Q, Ji S, Yue Q, Wang L, Liu J, Jia J. *Anal. Chem.*, **2009**, 81(13): 5381–5389
- [10] Li P, Zhang W, Zhao J, Meng F, Yue Q, Wang L, Li H, Gu X, Zhang S, Liu J. *Analyst*, **2012**, 137(18): 4318–4326
- [11] Ma W, Han D, Gan S, Zhang N, Liu S, Wu T, Zhang Q, Dong X, Niu L. *Chem. Commun.*, **2013**, 49(71): 7842–7844
- [12] Ma W, Han D, Zhang N, Li F, Wu T, Dong X, Niu L. *Analyst*, **2013**, 138(8): 2335–2342
- [13] Ma W, Han D, Zhou M, Sun H, Wang L, Dong X, Niu L. *Chem. Sci.*, **2014**, 5(10): 3946–3951
- [14] Miller D M, Buettner G R, Aust S D. *Free Radic. Biol. Med.*, **1990**, 8(1): 95–108
- [15] Henle E S, Luo Y, Gassmann W, Linn S J. *Biol. Chem.*, **1996**, 271(35): 21177–21186
- [16] Podmore I D, Griffiths H R, Herbert K E, Mistry N, Mistry P, Lunec J. *Nature*, **1998**, 392(6676): 559
- [17] Nagaveni K, Hegde M S, Ravishankar N, Subbanna G N, Madras G. *Langmuir*, **2004**, 20(7): 2900–2907
- [18] O'Regan B, Gratzel M. *Nature*, **1991**, 353(6346): 737–740
- [19] Hagfeldt A, Gratzel M. *Chem. Rev.*, **1995**, 95(1): 49–68
- [20] Fujihara K, Ohno T, Matsumura M. *J. Chem. Soc. Faraday Trans.*, **1998**, 94: 3705–3709
- [21] Hoffmann M R, Martin S T, Choi W, Bahnemann D W. *Chem. Rev.*, **1995**, 95(1): 69–96
- [22] Zhou X, Dong S S, Dong S S, Liu Y H, Wan L D. *Chin. J. Lumin.*, **2015**, 36(7): 769–774
- [23] Ishibashi K, Fujishima A, Watanabe T, Hashimoto K. *Electrochem. Commun.*, **2000**, 2(3): 207–210
- [24] Moser J, Punchedewa S, Infelta P P, Gratzel M. *Langmuir*, **1991**, 7(12): 3012–3018
- [25] Nosaka Y, Komori S, Yawata K, Hirakawa T, Nosaka A Y. *Phys. Chem. Chem. Phys.*, **2003**, 5(20): 4731–4735
- [26] Ishibashi K, Fujishima A, Watanabe T, Hashimoto K. *J. Photochem. Photobiol. A*, **2000**, 134(1-2): 139–142